EVOLUTIONARY BIOLOGY

A substitution in the glutathione reductase lowers electron leakage and inflammation in modern humans

Lucia Coppo[1]*†, Pradeep Mishra[1]†‡, Nora Siefert[1], Arne Holmgren[1]§, Svante Pääbo[2,3]*, Hugo Zeberg[2,4]*

Glutathione reductase is a critical enzyme for preventing oxidative stress and maintaining a reduced intracellular environment. Almost all present-day humans carry an amino acid substitution (S232G) in this enzyme relative to apes and Neanderthals. We express the modern human and the ancestral enzymes and show that whereas the activity and stability are unaffected by the amino acid substitution, the ancestral enzyme produces more reactive oxygen species and increases cellular levels of transcripts encoding cytokines. We furthermore show that the ancestral enzyme has been reintroduced into the modern human gene pool by gene flow from Neanderthals and is associated with multiple traits in present-day people, including increased susceptibility for inflammatory-associated disorders and vascular disease.

INTRODUCTION

Aerobic organisms face the challenge of oxidative damage caused by reactive oxygen species produced as metabolic by-products. One evolutionarily conserved mechanism for preventing oxidative damage is glutathione, which, after becoming oxidized by oxygen radicals, is recycled to the reduced form by glutathione reductase (GR). This enzyme is present in the cytosol, in mitochondria (*1*, *2*), and extracellularly (*3*). During the recycling, an electron is transferred from an enzyme cofactor to the oxidized glutathione. However, in the absence of oxidized glutathione (GSSG), GR can paradoxically generate reactive oxygen species by transferring electrons to oxygen instead (*4*). Here, we describe a functionally relevant change in GR on the evolutionary lineage leading to modern humans.

The closest evolutionary relatives of present-day humans, Neanderthals and Denisovans, so-called "archaic" humans, shared an ancestral population with the ancestors of modern humans about half a million years ago (*5*). Three Neanderthal genomes (*5*–*7*) and one Denisovan genome (*8*) have been sequenced to high quality. This makes it possible to identify genetic changes that characterize modern humans. Among the single-nucleotide substitutions on the lineage leading to modern humans, which alter protein sequences, approximately 100 are known to occur among all or almost all humans today but not in the archaic genomes available to date (*9*). One of these affects GR, which, in present-day humans, carries a glycine residue at position 232, whereas Neanderthals, Denisovans, and other primates carry a serine residue at this position. Note that position 232 in the nascent protein sequence corresponds to position 189 after cleavage of the mitochondrial signal peptide.

When modern humans encountered Neanderthals after leaving Africa, the two groups mixed, and as a result, some Neanderthal DNA variants were introduced into the gene pool of modern humans where they persist until today (*10*). Thus, some ancestral genetic variants and some genetic variants unique to Neanderthals exist among present-day people, often at low frequencies. Here, we show that one such variant encodes the ancestral form of GR. We describe the properties of the ancestral and modern human enzymes as well as the effects on the carriers of these variants today.

RESULTS

Enzymology

To characterize the functional consequences of the S232G substitution, we expressed and purified the modern human and Neanderthal (ancestral) forms of GR (fig. S1). GR catalyzes the reduction of GSSG [glutathione disulfide (GSSG)] using NADPH (nicotinamide adenine dinucleotide phosphate) as an electron donor. We measured the specific activity of GR in the presence of GSSG by monitoring NADPH consumption through the decrease of its absorption at 340 nm upon oxidation to $NADP^+$. We find no difference in the kinetics of the Neanderthal and modern human variants of the enzyme (Fig. 1A, table S1, and fig. S2). We further assessed the thermal stability of GR in the absence and presence of NADPH and GSSG, respectively, and found similar stabilities for two forms of the enzyme (Fig. 1, B and C). Moreover, the two variants of the enzyme bound the same amount of flavin adenine dinucleotide (FAD) (table S2).

As mentioned above, GR transfers electrons from NADPH to oxygen in the absence of its physiological substrate, GSSG, thus generating superoxide ($O_2^{\bullet-}$) (*4*, *11*). In an aqueous environment, this leakage of electrons then results in the generation of hydrogen peroxide. In a healthy cell, there are minimal amounts of GSSG, with concentrations of reduced glutathione (GSH) being 100-fold higher than the concentration of GSSG, whereas under oxidative stress, the molar ratio GSH:GSSG is reduced to values of 10:1 and even 1:1 (*12*). To test the extent to which the ancestral and modern human forms of GR may leak electrons, we measured the decrease in absorbance of NADPH at 340 nm in the absence of GSSG. We found that the rate of NADPH consumption for the modern human GR is ~40% of that of the Neanderthal GR ($P = 0.023$; Fig. 1D). Thus, in the absence of GSSG, Neanderthal and Denisovan GRs leak electrons to a higher

[1]Division of Biochemistry, Department of Medical Biochemistry and Biophysics, Karolinska Institutet, SE-17165 Stockholm, Sweden. [2]Max Planck Institute for Evolutionary Anthropology, Deutscher Platz 6, D-04103 Leipzig, Germany. [3]Okinawa Institute of Science and Technology, Onna-son, Okinawa 904-0495, Japan. [4]Department of Neuroscience, Karolinska Institutet, SE-17165 Stockholm, Sweden.
*Corresponding author. Email: lucia.coppo@ki.se (L.C.); paabo@eva.mpg.de (S.P.); hugo.zeberg@ki.se (H.Z.)
†These authors contributed equally to this work.
‡Present address: Department of Medical Biochemistry and Biophysics, Umeå University, 90187 Umeå, Sweden.
§Deceased.

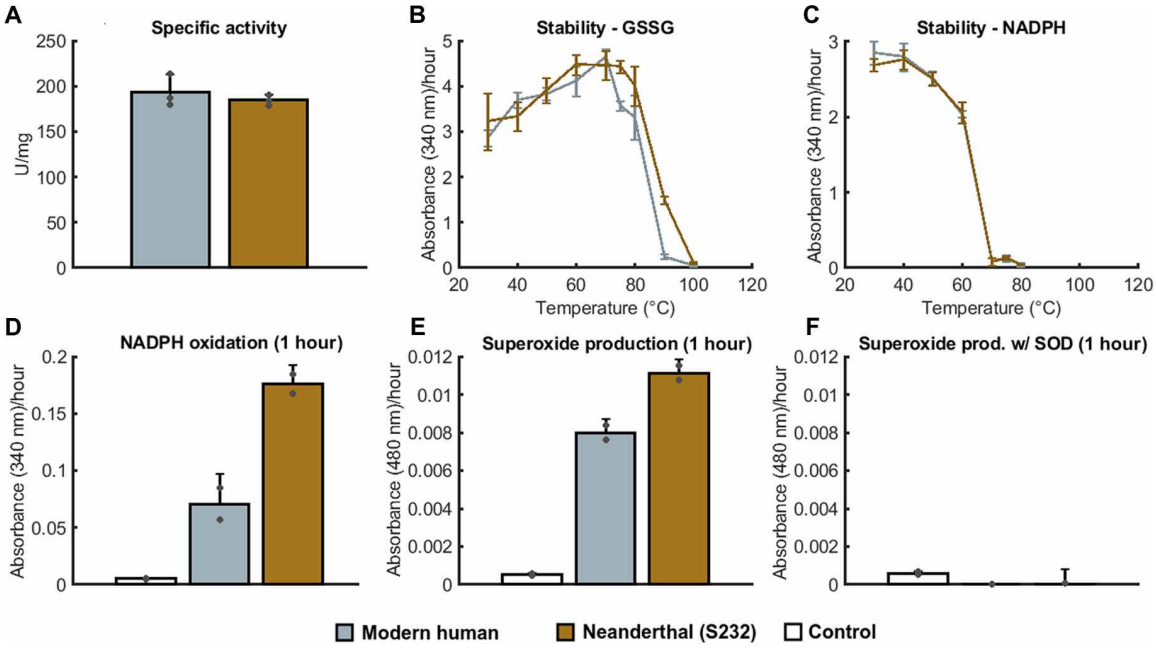

Fig. 1. Characterization of the modern human and Neanderthal variant of GR. (**A**) Specific activity in the presence of NADPH and GSSG. (**B** and **C**) Stability of the enzyme as a function of temperature in the presence of GSSG or NADPH, respectively. (**D**) NADPH oxidation under aerobic conditions, measured as loss of absorbance for NADPH when 1 μM of each enzyme was mixed with 200 μM NADPH. The oxidation of NADPH for the modern human variant is 40% of oxidation for the Neanderthal variant ($P = 0.023$). (**E**) NADPH oxidation resulted in the production of superoxide ($O_2^{\bullet-}$), measured as absorbance for adrenochrome, which is produced when superoxide reacts with epinephrine. The modern human GR variant produces 71% of the superoxide that the Neanderthal variant produces ($P = 0.028$). (**F**) Same as (E), but in the presence of superoxide dismutase. Error bars indicate 95% confidence intervals. Control without GR.

extent than the modern human GR. We verified that the consumption of NADPH leads to the production of superoxide by measuring the conversion of epinephrine to adrenochrome (*13*) and showing that this is abolished by the addition of superoxide dismutase (Fig. 1, E and F).

Neanderthal introgression

The S232G substitution is caused by an A-to-G nucleotide substitution at position 32,888 (RefSeq NG_027719.1) on the coding strand of *GSR*, the gene encoding GR. We next investigated whether this substitution occurs in all present-day humans. Among the individuals in the 1000 Genomes Project (*14*), the ancestral T allele on the noncoding strand (chr8: 30,557,599; hg19) occurs at a carrier frequency of 1.0 to 3.9% in Indian populations, 3.5% in Bangladeshis, 1.0% in Sri Lankan Tamils, and 1.0% in Puerto Ricans, while it is missing in other 1000 Genomes populations (Fig. 2A and table S3).

In the chromosomal region surrounding position 32,888, carriers of the ancestral allele carry nucleotide variants that match the genome of an approximately 45,000-year-old Neanderthal from Vindija Cave in Croatia. This pattern extends 66,705 base pairs (bp) upstream and 222,685 bp downstream (chr8: 30,334,914 to 30,624,304) of the missense variant. Chromosomal segments displaying similarity to Neanderthals may either have entered the modern human genome pool by gene flow when the two groups met between 40,000 and 100,000 years ago (Fig. 2B) or derive from the common ancestors of the two groups that existed about half a million years ago. Given the recombination rate of the region (*15*) and conservative assumptions about generation length of ancient humans, the time of lineage split between modern humans and Neanderthals, and the age of the Neanderthal specimen (*16*), the length of the region is incompatible with this region having existed in the two groups because they diverged from each other ($P = 9.5 \times 10^{-5}$). We thus conclude that the *GSR* variant encoding the ancestral form of the enzyme comes from gene flow from Neanderthals.

Nucleotide variants in the haplotype carrying the ancestral missense variant (Fig. 2C) match the genome of the Neanderthal from the Vindija Cave more closely than two Neanderthals and a Denisovan from southern Siberia (93.8% of the alleles in $r^2 > 0.8$ match the Vindija Neanderthal genome, whereas 75.0, 65.0, and 35.0% match the Altai Neanderthal, Chagyrskaya Neanderthal, and Denisovan genomes, respectively). This is in agreement with gene flow from Neanderthals into modern humans having occurred mainly from Neanderthal populations related closer to the Croatian Neanderthals than to other Neanderthals studied to date (*6*, *7*). In the genomic region harboring the Neanderthal haplotype, we find four human-derived (*17*) intronic variants in *GSR* in addition to the missense variant (table S4).

Phenotypic effects in humans

We found the Neanderthal-derived GR variant in the UK Biobank [~0.6 per mil (‰)], in the FinnGen Biobank (~4.8‰), and in the Michigan Genomics Initiative (~2.2‰) but not in Biobank Japan or the Million Veterans Program and performed a phenome-wide scan for associations in each of the three former biobanks. In the Michigan Genomics Initiative cohort, we detected a single phenome-wide significant ($P < 2.8 \times 10^{-5}$) association with "Disorders involving the immune mechanism" [odds ratio (OR) = 27.1, 95% confidence interval (CI) = 6.2 to 117.9, $P = 1.1 \times 10^{-5}$; Fig. 3A]. This phenotype is not scored in FinnGen, and the number of cases was too low in the UK Biobank ($n = 249$, c.f. $n = 1884$ for Michigan Genomics Initiative) to detect a signal.

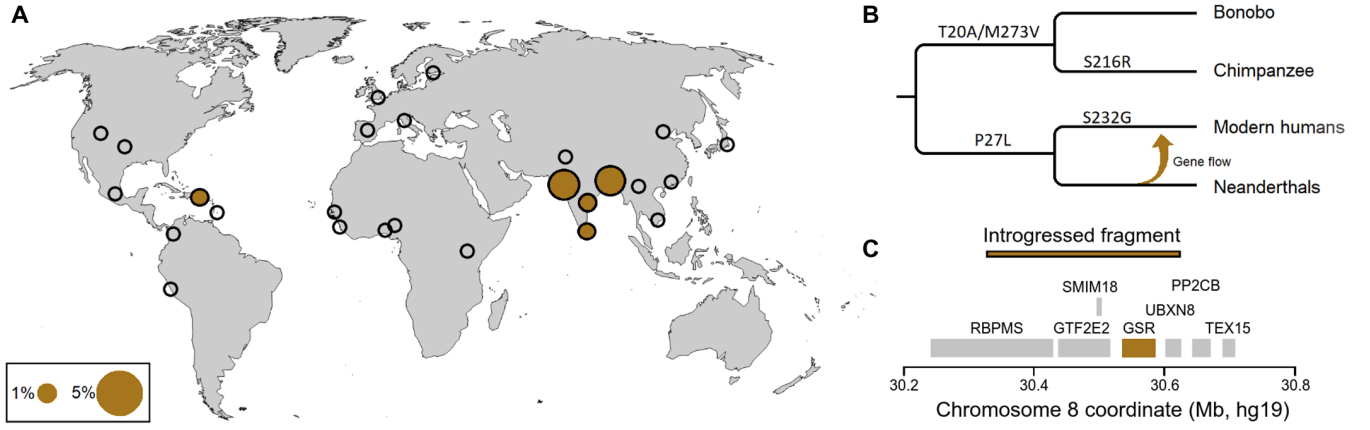

Fig. 2. Geographical distribution, human and ape amino acid replacements in GR, and introgressed fragment. (**A**) Allele frequency of S232 in 26 populations from the 1000 Genomes Project. S232 is mainly present on the Indian subcontinent. Black circle indicates population without the S232 allele. Gold disk indicates the allele frequency with the scale as shown. (**B**) Amino acid replacements in GR among humans and apes. The ancestral S232 was reintroduced into modern humans. (**C**) Genomic region of the introgressed haplotype encoding S232.

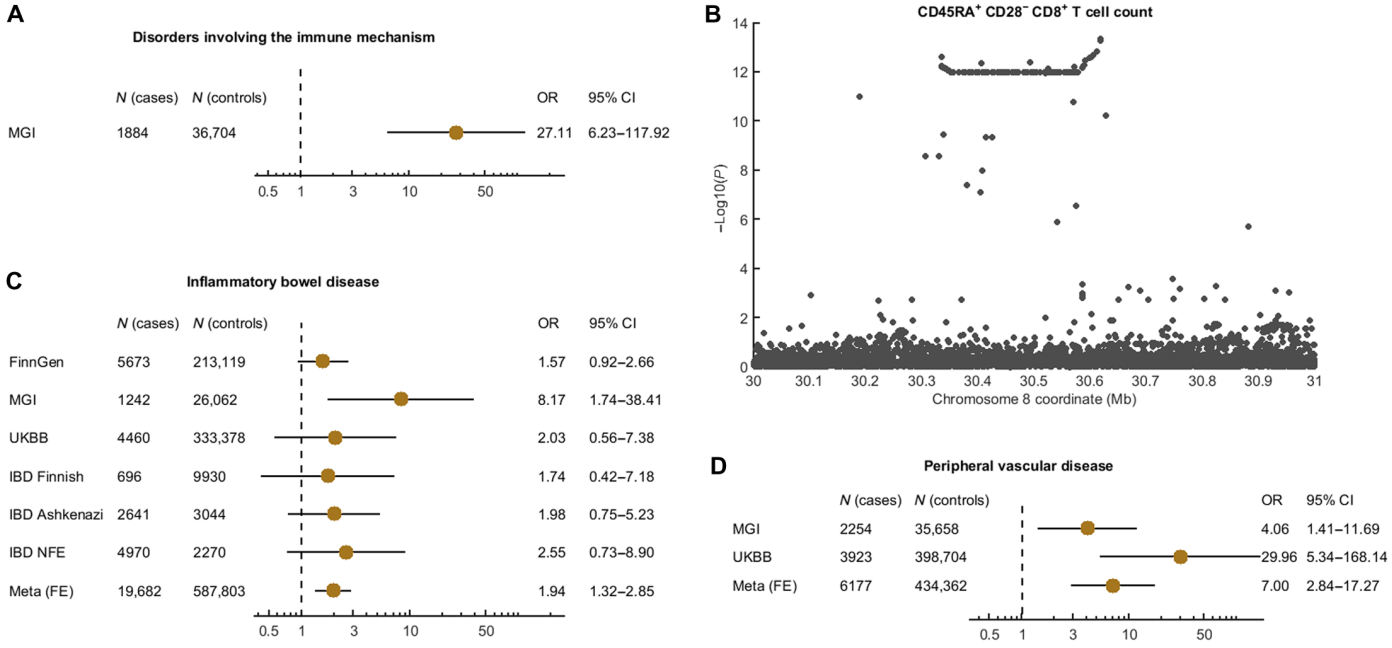

Fig. 3. Phenotypic effects of the Neanderthal GR variant. (**A**) A phenome-wide significant association with the ancestral S232 in Michigan Genomics Initiative (MGI) showing increased susceptibility to disorders involving the immune mechanism ($P = 1.1 \times 10^{-5}$). (**B**) The Neanderthal haplotype is associated with an increased count of TEMRA cells ($CD45RA^+ CD28^- CD8^+$). (**C**) Carriers of S232 have an increased risk of IBD in three biobanks and three study populations from the IBD Exomes Portal ($P = 7.0 \times 10^{-4}$). "NFE" denotes Non-Finnish Europeans, and "Meta (FE)" denotes a fixed-effect meta-analysis by inverse-variance weighting. (**D**) S232 is a genetic risk factor for peripheral vascular disease in two cohorts ($P = 2.3 \times 10^{-5}$).

To shed light on the physiological connection between the S232 residue in GR and the immune system, we search for associations in a recent dataset of 731 immune cell traits in 3757 Sardinians (*18*). We find that carriers of the Neanderthal allele have ~4 times higher numbers of $CD45RA^+ CD28^- CD8^+$ T cells in the blood ($\beta = 301$, 95% CI = 219 to 383, $P = 1.0 \times 10^{-12}$; Fig. 3B), an association that is significant on the genome- and phenome-wide level ($P < 6.8 \times 10^{-11}$). These "terminally differentiated effector memory cells reexpressing CD45RA" (TEMRA) (*19*) are involved in chronic immunological disorders such as graft-versus-host disease (*20*), chronic hepatitis C infection (*21*), and inflammatory bowel disease (IBD) (*22*). It is plausible that TEMRA cells may be increased in carriers of the Neanderthal GR due to increased oxidative stress.

Because oxidative stress is involved in multiple diseases (*23*), we investigated other associations with disease in the biobanks where the S232 residue occurs. The most significant association of S232G with diseases in the UK Biobank is with "Peripheral vascular disease" (OR = 29.96, 95% CI = 5.34 to 168.14, $P = 1.4 \times 10^{-4}$), a disease

known to be associated with oxidative stress (*24*). This association is seen also in the Michigan Genomic Initiative biobank (OR = 4.06, 95% CI = 1.41 to 11.69, $P = 7.5 \times 10^{-3}$), and a combination of the two cohorts results in phenome-wide significant ($P < 3.7 \times 10^{-5}$) risk increase for carriers of the ancestral allele (Fig. 3D, OR = 7.01, 95% CI = 2.84–17.27, $P = 2.3 \times 10^{-5}$) (this phenotype was not scored in FinnGen).

Oxidative stress is also part of the pathophysiology of IBD (*25*, *26*) and the ileum mucosa of IBD patients has markedly low GSH:GSSG ratios (*26*). We therefore investigated the association between S232 and IBD in the three biobanks where it occurs. The Neanderthal-like ancestral allele increases the risk for IBD (Fig. 3C), and a meta-analysis shows that carriers of the Neanderthal allele are almost twice as likely to suffer from IBD relative to noncarriers (OR = 1.89, 95% CI = 1.18 to 3.01, $P = 7.8 \times 10^{-3}$). In the IBD Exomes Portal that combines data from three populations where IBD has been studied, a similar increase in risk is seen (OR = 1.87, 95% CI = 1.33 to 2.64, $P = 0.049$). A meta-analysis of the six study populations strengthens the association (OR = 1.94, 95% CI = 1.32 to 2.85, $P = 7.0 \times 10^{-4}$).

Phenotypic effects in cells

A possible functional link between the higher oxidative potential of the ancestral GR and inflammatory conditions is the production of cytokines, which mediate inflammatory responses and are induced by oxidative stress (*23*). We examined whether the ancestral GR, which produces more reactive oxygen species, may induce more inflammatory cytokines and chemokines compared to the modern human GR, when coincubated with either of two cell lines: Jurkat (human T lymphocytes) and CHME3 (human microglia). We added the two forms of GR to the culture medium at a physiological concentration (2.5 U/ml) for 24 hours and measured the levels of mRNAs encoding nuclear factor κB (NF-κB), which is involved in the transcription of many cytokines, and tumor necrosis factor–α (TNF-α), interleukin-1β (IL-1β), and IL-6, three mediators of the inflammatory response, by reverse transcription and quantitative polymerase chain reactions (RT-PCR). As expected, adding Neanderthal GR to the medium resulted in the production of more hydrogen peroxide than adding modern human GR ($P = 3.5 \times 10^{-4}$ and $P = 1.0 \times 10^{-4}$ for Jurkat and CHEM3, respectively) (Fig. 4, A and B). In Jurkat T cells, transcript levels of TNF-α were 47% higher ($P = 0.017$) when the medium was supplemented with the ancestral, Neanderthal-like GR compared to when it was supplemented with the modern human GR (Fig. 4C). In microglial CHME3 cells, levels of mRNAs encoding NF-κB were 57% higher in the presence of the ancestral GR than in the presence of the modern variant of GR ($P = 0.036$; Fig. 4F). A joint analysis of TNF-α and NF-κB in both Jurkat T cells and microglia CHME3 cells revealed a general effect of the Neanderthal variant ($P = 0.036$) compared to the modern human GR. This suggests that the higher oxidative stress caused by Neanderthal GR may have direct effects on cytokine production in immune cells, which may contribute to its association with diseases with an inflammatory component.

DISCUSSION

The S232G amino acid substitution in GR is present in almost all humans today. We here show that it causes the enzyme to leak fewer electrons, resulting in lower levels of oxidative stress. We note that in the quaternary structure of the protein, the S232G amino acid substitution is in the proximity of the NADPH-binding site (positions 232 to 243), compatible with an effect on electron leakage.

The expression of *GSR* could also potentially differ between Neanderthals and modern humans. One of the human-derived intronic variants in *GSR* (rs8191007; table S4), which falls between the 9th and the 10th exon of *GSR*, has some regulatory potential based on chromatin accessibility and a predicted transcription factor

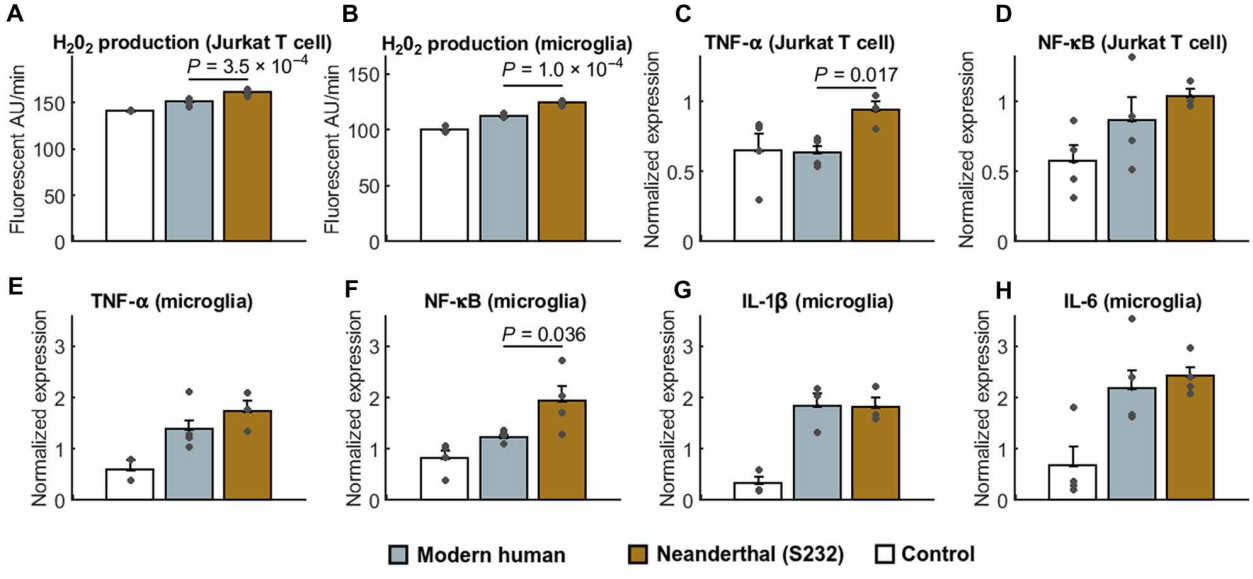

Fig. 4. Extracellular production of reactive oxygen species and transcriptional consequences. (**A** and **B**) Production of reactive oxygen species in the extracellular medium of Jurkat T cells or microglia cells (*CHME3*) in medium supplemented with the modern human or Neanderthal GR variants (2.5 U/ml) or in medium without GR (control). AU, arbitrary units. (**C** to **H**) mRNA expression in Jurkat or CHME3 cells after 24-hour exposure to modern human or Neanderthal GR variants. Normalized to expression in cells treated with lipopolysaccharide (10 ng/ml) for 4 hours. Error bars indicate SEM.

binding site (*27*). However, because the expression of *GSR* does not differ significantly between humans and apes or macaques (*28*), there is little reason to assume that expression of *GSR* would differ between modern humans and Neanderthals.

As a result of gene flow from Neanderthals, the ancestral GR version occurs on the Indian subcontinent at an allele frequency of 1 to 2% and at very low levels in Europe. By analyzing phenotypes with high prevalence in multiple large cohorts, we detect associations between the ancestral variant and vascular disease and IBD, despite its low allele frequency. Both these disorders have well-established links to oxidative stress and the immune response. In vascular disease, overproduction of reactive oxygen species causes vascular inflammation (*24*), and GSH deficiency characterizes the intestinal mucosal of patients with IBD (*26*, *29*). However, given that GR is ubiquitously expressed and that oxidative stress is involved in many diseases, the S232G amino acid replacement might have protective effects in addition to those described here. It may also affect traits such as aging. We can only speculate about any putative evolutionary advantage conferred by this variant upon modern humans in the past.

MATERIALS AND METHODS

Experimental design

Recombinant GR expression and purification

The plasmid pD441-H6SUMO-hGR expressing wild-type human GR with an N-terminal His-6-SUMO tag was obtained from Q. Cheng and E. S. J. Arnér (Karolinska Institutet) and was mutagenized at position 189 in the inferred protein using the primers GTAGGTCTCCTGCCTAGCCGTAGCGTTATTGTTGGTGCAG-3′ and GTAGGTCTCAGGCAGTTCTTCCAGCTGAAAAAAACC-3′. Initial denaturation at 95°C for 30 s was followed by 30 cycles of 10 s at 95°C, 30 s at 54°C, and 3 min at 72°C. The PCR product was digested with Eco31 I and Dpn I at 37°C for 1 hour. T4 DNA ligase was used to ligate the digested PCR product, and the ligation mixture was transformed into competent *Escherichia coli* DH5α cells and grown on kanamycin plates. The presence of the desired mutation was confirmed by DNA sequencing.

Plasmids were transformed into *E. coli* (Turbo Competent, New England Biolabs) and a single colony grown overnight in 10 ml of Terrific Broth media, containing kanamycin (100 μg/ml) and glycerol (8 g/liter) and was grown under agitation to A_{600} (absorbance at 600 nm) of 0.6 to 0.8. Then, 0.5 mM isopropyl-1-thio-β-D-galactopyranoside was added followed by incubation overnight at 24°C. Cells were pelleted; lysed in 100 mM Hepes (pH 7.5), 10% glycerol, 300 mM NaCl, and cOmplete EDTA-free Protease Inhibitor Cocktail (Sigma-Aldrich) at 4°C; sonicated using a Sonics Vibra Cell CV33; and centrifuged at 16,000 RPM for 30 min at 4°C. The lysate was loaded onto an immobilized metal affinity chromatography (IMAC) Nickel Sepharose column and eluted by Hepes buffer containing 100 mM imidazole. The His6-SUMO-tag was cleaved by ULP1 (SUMO protease), and the protein was collected in the flow-through from a second IMAC column, concentrated on 30-kDa Amicon centrifugal filters and stored in TE buffer containing 20% glycerol at −20°C.

Enzyme characterization

The apoenzyme precipitation and reconstitution followed (*30*), and concentration was measured by absorbance at A_{278} and 57,000 M^{-1} cm^{-1} as extinction coefficient. Protein concentrations were determined spectrophotometrically by FAD absorption at 460 nm (ϵ = 11,300 M^{-1} cm^{-1}; one FAD assumed to correspond to one GR subunit) in phosphate-buffered saline (PBS) (Thermo Fisher Scientific), 2 mM EDTA, and BSA (bovine serum albumin; 0.05 mg/ml; Sigma-Aldrich). Absorbance spectra between 300 and 700 nm were recorded in 1-ml quartz cuvettes in a Tecan Infinite M200 Pro plate reader. To measure the specific activity, 1 nM modern human GR or 1 nM Neanderthal GR was dissolved in the assay buffer [PBS, 2 mM EDTA, and BSA (0.05 mg/ml)] with 300 μM NADPH. NADPH absorbance was standardized by the absorbance at 340 nm before each sample. The reaction was started by adding GSSG to a final concentration of 1 mM, and the reduction of GSSG was determined indirectly by the consumption of NADPH. One unit of enzyme activity is defined as the reduction of 1 μmol of GSSG per minute per milligram of GR at 25°C. We tested which incubation temperature between 30° and 90°C leads to 50% enzyme inactivation in 10 min after the addition of 200 μM NADPH or 1 mM GSSG and recording of the absorbance at 340 nm every 20 s for 5 min. To test the oxidation of NADPH by GRs in the absence of GSSG, 1 μM enzyme was mixed with 200 μM NADPH at 37°C, and the absorbance at 340 nm was recorded every 30 s for 1 hour. Superoxide production was also assessed in reactions containing 2 mM epinephrine, and adrenochrome production was measured by absorbance at 480 nm. Addition of an excess of superoxide dismutase (6 U per well) completely abolished the adrenochrome formation, confirming that superoxide was formed. K_M and V_{max} for NADPH were estimated in 200-μl volumes containing 1 nM enzyme and 7.5 to 50 μM NADPH concentrations, starting the reactions by the addition of 1 mM GSSG. To determine K_M and V_{max} for GSSG, reactions contained 200 μM NADPH, 1 nM enzyme, and 10 to 640 μM GSSG concentrations and were started by adding 200 μM NADPH.

Cell culture experiments

CHME3 and Jurkat cells were maintained in a DMEM (Dulbecco's modified Eagle's medium; Lonza) and RPMI 1640 (Merck) medium, respectively, supplemented with 10% fetal bovine serum, at 37°C and 5% CO_2. Viability was measured in 96-well culture plates (7000 cells per well) with 3-(4,5-dimethylthiazol-2-yl)-2,5-diphenyl tetrazolium bromide (Sigma-Aldrich) and absorbance at 570 nm as previously described (*31*). For mRNA isolation, 400,000 CHME3 cells or 200,000 Jurkat cells were plated in six-well plates. The next day, modern human GR or Neanderthal GR (2.5 U/ml) was added. Each well was washed twice with PBS, and cells were collected in 200 μl of TRIzol (Life Technologies) and reverse-transcribed using Maxima First Strand cDNA synthesis kit (Thermo Fisher Scientific). Quantification of IL-1 and IL-6, TNF-α, and NF-κB mRNA levels was assessed by real-time RT-PCR using the primers in table S5. Relative expression was calculated using the ΔΔCT (delta-delta cycle threshold) method after normalizing to actin expression and normalized to lipopolysaccharide (10 ng/ml) treatment.

Measurement of H_2O_2 in the cell medium was carried out as previously described (*32*). Briefly, final concentrations of 50 μM Amplex Red and horseradish peroxidase (0.1 U/ml) were added to Jurkat or CHME3 cell medium, respectively, and fluorescence was monitored (560 nm excitation/590 nm emission) for 1 hour.

Evidence for introgression

The S232G polymorphism sits on a 289.4-kb haplotype (r^2 > 0.8 in all 1000 Genomes individuals) defined by 46 private single-nucleotide polymorphisms on the Neanderthal lineage (i.e., the Neanderthal allele is missing in 108 Yoruba individuals, and Yoruba carry the ancestral allele) with coordinates chr8: 30,334,914 to 30,624,304 (hg19). Using this length, a local recombination rate of 0.34 cM/Mb

(deCODE) (*15*), the parameters from (*33*), and the formula derived by Huerta-Sánchez *et al.* (*16*) yields a probability of $P = 9.5 \times 10^{-5}$ for incomplete lineage sorting.

Phenotypic consequences of S232

We searched for carriers of the S232 allele (T at rs8190976) in the UK Biobank, FinnGen, the Michigan Genomics Initiative, the Million Veterans' Program, and Biobank Japan. We found carriers of the minor allele at rs8190976 in the UK BioBank and in the Michigan Genomics Initiative. In FinnGen, we found carriers of the minor allele of rs376850387, which is in perfect linkage disequilibrium ($r^2 = 1$) with rs8190976 in the 1000 Genomes Project (*14*) and was used as a proxy, whereas rs8190976 was present in IBD Exomes Portal.

Statistical analysis

Comparisons between groups were made by two-tailed unpaired *t* tests. The joint analysis of TNF-α and NF-κB in both Jurkat T cells and microglia CHME3 cells was performed using a two-way analysis of variance (ANOVA). The Michaelis-Menten equations were calculated using GraphPad Prism Software (GraphPad Software Inc., La Jolla, CA), as well as the thermal stabilities. The expected length of a shared ancestral sequence was assumed to follow a Gamma distribution, as previously described (*16*). Meta-analyses of phenotypic effects were done using the inverse variance method.

SUPPLEMENTARY MATERIALS

Supplementary material for this article is available at https://science.org/doi/10.1126/sciadv.abm1148

View/request a protocol for this paper from *Bio-protocol*.

REFERENCES AND NOTES

1. M. J. Kelner, M. A. Montoya, Structural organization of the human glutathione reductase gene: Determination of correct cDNA sequence and identification of a mitochondrial leader sequence. *Biochem. Biophys. Res. Commun.* **269**, 366–368 (2000).
2. M. Taniguchi, T. Hara, H. Honda, Similarities between rat liver mitochondrial and cytosolic glutathione reductases and their apoenzyme accumulation in riboflavin deficiency. *Biochem. Int.* **13**, 447–454 (1986).
3. C. Manso, F. Wroblewski, Glutathione reductase activity in blood and body fluids. *J. Clin. Invest.* **37**, 214–218 (1958).
4. K. Anestål, E. S. J. Arnér, Rapid induction of cell death by selenium-compromised thioredoxin reductase 1 but not by the fully active enzyme containing selenocysteine. *J. Biol. Chem.* **278**, 15966–15972 (2003).
5. K. Prüfer, F. Racimo, N. Patterson, F. Jay, S. Sankararaman, S. Sawyer, A. Heinze, G. Renaud, P. H. Sudmant, C. de Filippo, H. Li, S. Mallick, M. Dannemann, Q. Fu, M. Kircher, M. Kuhlwilm, M. Lachmann, M. Meyer, M. Ongyerth, M. Siebauer, C. Theunert, A. Tandon, P. Moorjani, J. Pickrell, J. C. Mullikin, S. H. Vohr, R. E. Green, I. Hellmann, P. L. F. Johnson, H. Blanche, H. Cann, J. O. Kitzman, J. Shendure, E. E. Eichler, E. S. Lein, T. E. Bakken, L. V. Golovanova, V. B. Doronichev, M. V. Shunkov, A. P. Derevianko, B. Viola, M. Slatkin, D. Reich, J. Kelso, S. Pääbo, The complete genome sequence of a Neanderthal from the Altai Mountains. *Nature* **505**, 43–49 (2014).
6. K. Prüfer, C. de Filippo, S. Grote, F. Mafessoni, P. Korlević, M. Hajdinjak, B. Vernot, L. Skov, P. Hsieh, S. Peyrégne, D. Reher, C. Hopfe, S. Nagel, T. Maricic, Q. Fu, C. Theunert, R. Rogers, P. Skoglund, M. Chintalapati, M. Dannemann, B. J. Nelson, F. M. Key, P. Rudan, Ž. Kućan, I. Gušić, L. V. Golovanova, V. B. Doronichev, N. Patterson, D. Reich, E. E. Eichler, M. Slatkin, M. H. Schierup, A. M. Andrés, J. Kelso, M. Meyer, S. Pääbo, A high-coverage Neandertal genome from Vindija Cave in Croatia. *Science* **358**, 655–658 (2017).
7. F. Mafessoni, S. Grote, C. de Filippo, V. Slon, K. A. Kolobova, B. Viola, S. V. Markin, M. Chintalapati, S. Peyrégne, L. Skov, P. Skoglund, A. I. Krivoshapkin, A. P. Derevianko, M. Meyer, J. Kelso, B. Peter, K. Prüfer, S. Pääbo, A high-coverage Neandertal genome from Chagyrskaya Cave. *Proc. Natl. Acad. Sci. U.S.A.* **117**, 15132–15136 (2020).
8. M. Meyer, M. Kircher, M.-T. Gansauge, H. Li, F. Racimo, S. Mallick, J. G. Schraiber, F. Jay, K. Prüfer, C. de Filippo, P. H. Sudmant, C. Alkan, Q. Fu, R. Do, N. Rohland, A. Tandon, M. Siebauer, R. E. Green, K. Bryc, A. W. Briggs, U. Stenzel, J. Dabney, J. Shendure, J. Kitzman, M. F. Hammer, M. V. Shunkov, A. P. Derevianko, N. Patterson, A. M. Andrés, E. E. Eichler, M. Slatkin, D. Reich, J. Kelso, S. Pääbo, A high-coverage genome sequence from an archaic Denisovan individual. *Science* **338**, 222–226 (2012).
9. S. Pääbo, The human condition-a molecular approach. *Cell* **157**, 216–226 (2014).
10. R. E. Green, J. Krause, A. W. Briggs, T. Maricic, U. Stenzel, M. Kircher, N. Patterson, H. Li, W. Zhai, M. H.-Y. Fritz, N. F. Hansen, E. Y. Durand, A.-S. Malaspinas, J. D. Jensen, T. Marques-Bonet, C. Alkan, K. Prüfer, M. Meyer, H. A. Burbano, J. M. Good, R. Schultz, A. Aximu-Petri, A. Butthof, B. Höber, B. Höffner, M. Siegemund, A. Weihmann, C. Nusbaum, E. S. Lander, C. Russ, N. Novod, J. Affourtit, M. Egholm, C. Verna, P. Rudan, D. Brajkovic, Ž. Kucan, I. Gušic, V. B. Doronichev, L. V. Golovanova, C. Lalueza-Fox, M. de la Rasilla, J. Fortea, A. Rosas, R. W. Schmitz, P. L. F. Johnson, E. E. Eichler, D. Falush, E. Birney, J. C. Mullikin, M. Slatkin, R. Nielsen, J. Kelso, M. Lachmann, D. Reich, S. Pääbo, A draft sequence of the Neandertal genome. *Science* **328**, 710–722 (2010).
11. P. Korge, G. Calmettes, J. N. Weiss, Increased reactive oxygen species production during reductive stress: The roles of mitochondrial glutathione and thioredoxin reductases. *Biochim. Biophys. Acta* **1847**, 514–525 (2015).
12. Y. C. Chai, S. S. Ashraf, K. Rokutan, R. B. J. Johnston, J. A. Thomas, S-thiolation of individual human neutrophil proteins including actin by stimulation of the respiratory burst: Evidence against a role for glutathione disulfide. *Arch. Biochem. Biophys.* **310**, 273–281 (1994).
13. D. L. Vander Jagt, L. A. Hunsaker, T. J. Vander Jagt, M. S. Gomez, D. M. Gonzales, L. M. Deck, R. E. Royer, Inactivation of glutathione reductase by 4-hydroxynonenal and other endogenous aldehydes. *Biochem. Pharmacol.* **53**, 1133–1140 (1997).
14. A. Auton, L. D. Brooks, R. M. Durbin, E. P. Garrison, H. M. Kang, J. O. Korbel, J. L. Marchini, S. McCarthy, G. A. McVean, G. R. Abecasis, A global reference for human genetic variation. *Nature* **526**, 68–74 (2015).
15. A. Kong, G. Thorleifsson, D. F. Gudbjartsson, G. Masson, A. Sigurdsson, A. Jonasdottir, G. B. Walters, A. Jonasdottir, A. Gylfason, K. T. Kristinsson, S. A. Gudjonsson, M. L. Frigge, A. Helgason, U. Thorsteinsdottir, K. Stefansson, Fine-scale recombination rate differences between sexes, populations and individuals. *Nature* **467**, 1099–1103 (2010).
16. E. Huerta-Sánchez, X. Jin, Asan, Z. Bianba, B. M. Peter, N. Vinckenbosch, Y. Liang, X. Yi, M. He, M. Somel, P. Ni, B. Wang, X. Ou, J. L. Huasang, Z. X. P. Cuo, K. Li, G. Gao, Y. Yin, W. Wang, X. Zhang, X. Xu, H. Yang, Y. Li, J. Wang, J. Wang, R. Nielsen, Altitude adaptation in Tibetans caused by introgression of Denisovan-like DNA. *Nature* **512**, 194–197 (2014).
17. K. L. Howe, P. Achuthan, J. Allen, J. Allen, J. Alvarez-Jarreta, M. R. Amode, I. M. Armean, A. G. Azov, R. Bennett, J. Bhai, K. Billis, S. Boddu, M. Charkhchi, C. Cummins, L. Da Rin Fioretto, C. Davidson, K. Dodiya, B. El Houdaigui, R. Fatima, A. Gall, C. Garcia Giron, T. Grego, C. Guijarro-Clarke, L. Haggerty, A. Hemrom, T. Hourlier, O. G. Izuogu, T. Juettemann, V. Kaikala, M. Kay, I. Lavidas, T. Le, D. Lemos, J. Gonzalez Martinez, J. C. Marugán, T. Maurel, A. C. McMahon, S. Mohanan, B. Moore, M. Muffato, D. N. Oheh, D. Paraschas, A. Parker, A. Parton, I. Prosovetskaia, M. P. Sakthivel, A. I. A. Salam, B. M. Schmitt, H. Schuilenburg, D. Sheppard, E. Steed, M. Szpak, M. Szuba, K. Taylor, A. Thormann, G. Threadgold, B. Walts, A. Winterbottom, M. Chakiachvili, A. Chaubal, N. De Silva, B. Flint, A. Frankish, S. E. Hunt, G. R. Ilsley, N. Langridge, J. E. Loveland, F. J. Martin, J. M. Mudge, J. Morales, E. Perry, M. Ruffier, J. Tate, D. Thybert, S. J. Trevanion, F. Cunningham, A. D. Yates, D. R. Zerbino, P. Flicek, Ensembl 2021. *Nucleic Acids Res.* **49**, D884–D891 (2021).
18. V. Orrù, M. Steri, C. Sidore, M. Marongiu, V. Serra, S. Olla, G. Sole, S. Lai, M. Dei, A. Mulas, F. Virdis, M. G. Piras, M. Lobina, M. Marongiu, M. Pitzalis, F. Deidda, A. Loizedda, S. Onano, M. Zoledziewska, S. Sawcer, M. Devoto, M. Gorospe, G. R. Abecasis, M. Floris, M. Pala, D. Schlessinger, E. Fiorillo, F. Cucca, Complex genetic signatures in immune cells underlie autoimmunity and inform therapy. *Nat. Genet.* **52**, 1036–1045 (2020).
19. A. Larbi, T. Fulop, From "truly naïve" to "exhausted senescent" T cells: When markers predict functionality. *Cytometry A* **85**, 25–35 (2014).
20. M. G. H. Betjes, R. W. J. Meijers, E. A. de Wit, W. Weimar, N. H. R. Litjens, Terminally differentiated CD8+ Temra cells are associated with the risk for acute kidney allograft rejection. *Transplantation* **94**, 63–69 (2012).
21. T. Shen, J. Zheng, C. Xu, J. Liu, W. Zhang, F. Lu, H. Zhuang, PD-1 expression on peripheral CD8+ TEM/TEMRA subsets closely correlated with HCV viral load in chronic hepatitis C patients. *Virol. J.* **7**, 310 (2010).
22. E. Lo Presti, R. Di Mitri, F. Mocciaro, A. B. Di Stefano, N. Scibetta, E. Unti, G. Cicero, G. Pecoraro, E. Conte, F. Dieli, S. Meraviglia, Characterization of γδ T cells in intestinal mucosa from patients with early-onset or long-standing inflammatory bowel disease and their correlation with clinical status. *J. Crohns Colitis* **13**, 873–883 (2019).
23. S. Reuter, S. C. Gupta, M. M. Chaturvedi, B. B. Aggarwal, Oxidative stress, inflammation, and cancer: How are they linked? *Free Radic. Biol. Med.* **49**, 1603–1616 (2010).
24. N. R. Madamanchi, A. Vendrov, M. S. Runge, Oxidative stress and vascular disease. *Arterioscler. Thromb. Vasc. Biol.* **25**, 29–38 (2005).
25. C. Costa Pereira, C. Durães, R. Coelho, D. Grácio, M. Silva, A. Peixoto, P. Lago, M. Pereira, T. Catarino, S. Pinho, J. P. Teixeira, G. Macedo, V. Annese, F. Magro, Association between polymorphisms in antioxidant genes and inflammatory bowel disease. *PLOS ONE* **12**, e0169102 (2017).
26. B. Sido, V. Hack, A. Hochlehnert, H. Lipps, C. Herfarth, W. Dröge, Impairment of intestinal glutathione synthesis in patients with inflammatory bowel disease. *Gut* **42**, 485–492 (1998).

27. S. Dong, A. P. Boyle, Predicting functional variants in enhancer and promoter elements using RegulomeDB. *Hum. Mutat.* **40**, 1292–1298 (2019).
28. E. Khrameeva, I. Kurochkin, D. Han, P. Guijarro, S. Kanton, M. Santel, Z. Qian, S. Rong, P. Mazin, M. Sabirov, M. Bulat, O. Efimova, A. Tkachev, S. Guo, C. C. Sherwood, J. G. Camp, S. Pääbo, B. Treutlein, P. Khaitovich, Single-cell-resolution transcriptome map of human, chimpanzee, bonobo, and macaque brains. *Genome Res.* **30**, 776–789 (2020).
29. F. Häuser, H. Rossmann, D. Laubert-Reh, P. S. Wild, T. Zeller, C. Müller, S. Neuwirth, S. Blankenberg, K. J. Lackner, Inflammatory bowel disease (IBD) locus 12: Is glutathione peroxidase-1 (GPX1) the relevant gene? *Genes Immun.* **16**, 571–575 (2015).
30. D. J. Worthington, M. A. Rosemeyer, Glutathione reductase from human erythrocytes. Molecular weight, subunit composition and aggregation properties. *Eur. J. Biochem.* **60**, 459–466 (1975).
31. X. Ren, S. M. Santhosh, L. Coppo, F. T. Ogata, J. Lu, A. Holmgren, The combination of ascorbate and menadione causes cancer cell death by oxidative stress and replicative stress. *Free Radic. Biol. Med.* **134**, 350–358 (2019).
32. U. Ermler, S. Ghisla, V. Massey, G. E. Schulz, Structural, spectroscopic and catalytic activity studies on glutathione reductase reconstituted with FAD analogues. *Eur. J. Biochem.* **199**, 133–138 (1991).
33. H. Zeberg, S. Pääbo, The major genetic risk factor for severe COVID-19 is inherited from Neanderthals. *Nature* **587**, 610–612 (2020).

Acknowledgments
Funding: This work was supported by NOMIS Foundation (to S.P.), Max Planck Society (to S.P.), Jeanssons Stiftelser (to H.Z.), and Magnus Bergvalls Stiftelse (to H.Z.). H.Z. is supported by the Swedish Research Council (2021-03050). **Author contributions:** Conceptualization: S.P. and H.Z. Methodology: A.H., S.P., and H.Z. Investigation: L.C., P.M., N.S., and H.Z. Supervision: S.P., A.H., and H.Z. Writing—original draft: H.Z. Writing—review and editing: H.Z. and S.P.
Competing interests: The authors declare that they have no competing interests. **Data and materials availability:** All data needed to evaluate the conclusions in the paper are present in the paper and/or the Supplementary Materials. The genomes for the 1000 Genomes Projects are available at www.internationalgenome.org/data, and the archaic genomes are available at http://cdna.eva.mpg.de/neandertal/. RegulomeDB can be found at https://regulomedb.org/. The UK Biobank and the Michigan Genomics Initiative (freeze 2) can be queried at https://pheweb.org/, whereas FinnGen (release 5) is accessible at https://r5.finngen.fi/, and the Inflammatory Bowel Disease Exomes Browser is accessible at https://ibd.broadinstitute.org/. The $CD45RA^+$ $CD28^-$ $CD8^+$ T cell data are deposited at www.ebi.ac.uk/gwas/studies/GCST90001698.

Submitted 26 August 2021
Accepted 10 November 2021
Published 5 January 2022
10.1126/sciadv.abm1148

ScienceAdvances

A substitution in the glutathione reductase lowers electron leakage and inflammation in modern humans

Lucia Coppo, Pradeep Mishra, Nora Siefert, Arne Holmgren, Svante Pbo, and Hugo Zeberg

Sci. Adv., **8** (1), eabm1148.
DOI: 10.1126/sciadv.abm1148

Science Advances (ISSN) is published by the American Association for the Advancement of Science. 1200 New York Avenue NW, Washington, DC 20005. The title *Science Advances* is a registered trademark of AAAS.